ACS Sustainable Chemistry & Engineering

Research Article

pubs.acs.org/journal/ascecg

Nanocomposite Catalyst with Palladium Nanoparticles Encapsulated in a Polymeric Acid: A Model for Tandem Environmental Catalysis

Tayirjan T. Isimjan,[†,⊥] Quan He,[†] Yong Liu,[†] Jesse Zhu,[†] Richard J. Puddephatt,*[,‡] and Darren J. Anderson[§]

[†]Department of Chemical Engineering, University of Western Ontario, London, Canada N6A 5B7

[‡]Department of Chemistry, University of Western Ontario, London, Canada N6A 5B7

[§]Vive Crop Protection, Toronto, Canada M5G 1Z6

ABSTRACT: The synthesis and characterization of a novel hybrid nanocomposite catalyst comprised of palladium nanoparticles embedded in polystyrene sulfonic acid (PSSH) and supported on metal oxides is reported. The catalysts are intended for application in green catalysis, and they are shown to be effective in the hydrolysis-reduction sequence of tandem catalytic reactions required for conversion of 2-phenyl-1,3-dioxolane to toluene or of phenol to cyclohexane. The two distinct components in the catalyst, Pd nanoparticles and acidic PSSH, are capable of catalyzing sequential reactions in one pot under mild conditions. This work has demonstrated a powerful approach toward designing high-performance, multifunctional, scalable, and environmentally friendly nanostructured tandem catalysts.

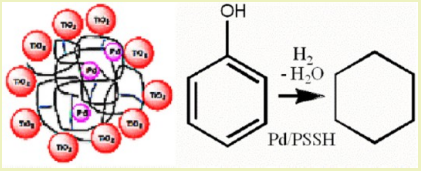

KEYWORDS: *Tandem catalyst, Palladium, Polystyrene sulfonic acid, Polyelectrolyte, Hydrolysis, Hydrogenation, Dehydration*

INTRODUCTION

There is great current interest in the development of tandem catalysis, which can bring about multistep synthetic processes in ways which are both environmentally friendly and economical. The term "tandem" indicates to that two or more reactions with distinct mechanisms occur sequentially in a single reaction vessel.[1,2] In general, there are two types of tandem catalytic systems: (1) one catalyst performs two or more reactions at a time[3−6] and (2) a combination of two or more catalysts is used to achieve the different transformations.[7,8] Tandem catalysis can dramatically simplify multiple catalytic transformations to a "one-pot" process, followed by a single workup stage, which minimizes solvent and energy use. This technique results in significantly decreased capital and operating costs associated with the production process and less waste formation.

The increasing popularity of tandem catalysis is highlighted by the large number of recent research reports in this area, especially involving catalysis by elemental palladium or palladium complexes.[1−21] Many of these reports describe the use of palladium complexes for cross-coupling reactions, combined with a second reaction in tandem. For instance, monometallic and dendritic SCS-pincer palladium complexes were used as catalysts in the catalytic autotandem reaction consisting of stannylation followed by an electrophilic addition.[13,14] An imidazolium-based ionic liquid has been used as solvent, stabilizer, and hydrogen transfer agent that leads efficiently to a Pd-catalyzed tandem coupling/reduction process.[15] A new synthetic route to *N*-aryl-2-benzylindolines from 2-allylanilines and two different aryl bromides is reported using a palladium based tandem catalyst in which two C−N bonds and one C−C bond were formed in a one-pot process.[21] There have been several reports on applications of polymer or dendrimer stabilized palladium nanocomposites, and some of them have been used in catalysts, membranes, and sensors.[22−32] However, in none of these cases has the polymer component of the nanocomposite been used as a catalytically active component.

In the present work, we have used a patented, inherently green synthesis process to produce a multifunctional nanocomposite catalyst.[33,34] This nanocomposite contains palladium nanoparticles, with mean diameter of 13 nm, and the strong acid polymer, polystyrene sulfonic acid (PSSH) embedded in a porous metal oxide support, which can be applied to facilitate tandem reactions. The Pd nanoparticles were used to catalyze a hydrogenation reaction while the strong acid polymers were used to sequentially catalyze both deprotection by hydrolysis and dehydration reactions in tandem. The catalytic activity of Pd/PSSH was evaluated in the conversion of 2-phenyl-1,3-dioxolane to toluene and in the conversion of phenol to cyclohexane, which are model reactions for the upgrading of oxygenates in biofuels. The catalyst has been designed to be environmentally friendly by concentration of the strong acid immediately adjacent to each palladium nanoparticle, thus avoiding the need for excess strong acid.

EXPERIMENTAL SECTION

Polystyrene sulfonic acid with molecular weight of 70 000, $NaBH_4$, 2-phenyl-1,3-dioxolane, benzaldehyde, benzyl alcohol, toluene, and TiO_2 were purchased from Aldrich. Palladium chloride with 99.9% purity (metal basis) was purchased from Alfa Aesar. Al_2O_3 was generously

Received: September 24, 2012
Revised: February 8, 2013
Published: February 20, 2013

provided by SASOL (Germany). All solvents were reagent grade and were used without further purification.

Synthesis of Palladium (Pd)/Polystyrene Sulfonic Acid (PSSH) Nanocomposite. A solution containing palladium(II) was obtained by dissolution of $PdCl_2$ (0.06 g) in aqueous H_2SO_4 (3 mL, 1 M), followed by dilution with water to a volume of 80 mL. This solution was added dropwise to a vigorously stirred (>800 rpm) aqueous solution of PSSH (80 mL, 2 mg/mL) by using a syringe pump (2 mL/min). The resulting clear, light yellow solution was subjected to 254 nm UV lamp for 1 h under vigorous stirring. The system was purged with N_2 for 30 min followed by the addition of $NaBH_4$ (64 mg, 1.7 mmol) in portions and the mixture was stirred for 1 h under N_2. The black solution was dialyzed and then freeze-dried to obtain the target composite: Pd/PSSH. The Pt/PSSH and Rh/PSSH catalysts were prepared in a similar way by using $PtCl_2$ or $RhCl_3$ in place of $PdCl_2$

Synthesis of Pd/PSSH Supported on TiO_2 and Al_2O_3. The Pd/PSSH nanocomposite was prepared in aqueous solution as described above. The solution was adjusted to pH of 8−9 and then TiO_2 or Al_2O_3 (3.2 g) was added in portions. The mixture was stirred for 2 h, followed by centrifugation and filtration. The solid was redispersed in H_2SO_4 (20 mL, 1 M) and then centrifuged, filtered, and dried to obtain the target composites: Pd/PSSH/TiO_2 or Pd/PSSH/Al_2O_3. The content of Pd in the catalysts was 0.8 wt % in both cases, as determined by ICP-AES.

Characterization. *Transmission Electron Microscopy (TEM).* TEM images of the catalysts were recorded by using a FEI TITAN 80-300 high resolution transmission electron microscope (HRTEM). Samples were prepared as follows: a small amount of the sample was suspended in distilled water, lightly sonicated, and a droplet placed on a porous carbon coated TEM grid made of Cu, dried in a desiccator overnight, and analyzed in the HRTEM at 300 keV.

Scanning Electron Microscopy (SEM). SEM images were captured using a model FIB/SEM LEO 1540XB microscope (Carl Zeiss, Oberkochen, Germany) operating at an electron beam voltage of 1 keV. Scaffolds were affixed to a carbon sample holder and coated with 4 nm osmium vapor before imaging. In addition, energy dispersive X-ray spectroscopy (EDX) was used to map the elemental composition and distribution within the nanocomposite.

X-ray Photoelectron Spectroscopy (XPS). The samples were characterized by using a Thermo Scientific K-Alpha XPS spectrometer (ThermoFisher, E. Grinstead, UK). The samples were run at a takeoff angle (relative to the surface) of 90°. A monochromatic Al Kα X-ray source was used, with a spot area (on a 90° sample) of 400 μm. Charge compensation was provided. Position of the energy scale was adjusted to place the main C 1s feature (C−C) at 285.0 eV. Survey spectra were obtained on each sample (pass energy 200 eV). Composition was obtained from separate spectra collected in a scanned mode (PE 150 eV). In addition, high resolution spectra were obtained in a scanned mode for just the requested peaks C, Pd + S (PE 25 eV).

Inductively Coupled Plasma (ICP). The sample was homogenized by using a vortex stirrer or manual shaking for at least 1 min. A known volume or weight of the sample was taken in a precleaned beaker, and the exact volume or weight of the sample was noted and then hot HNO_3 (2 mL, 69%) was added. The mixture was heated at 80−90 °C using a hot plate for 15−20 min after covering with a clean watch glass, cooled to room temperature and rinsed with another 2−3 mL of Milli-Q water. The mixture was filtered through a Whatman no. 41 filter paper into a known volumetric flask and the filter paper was rinsed twice with Milli-Q water. The resulting solution was then analyzed by ICP-OES (ICP-AES, Varian VISTA-Pro) against a known calibration standard. The result was computed and reported after subtraction from blank and taking dilution factor into consideration.

X-ray Powder Diffraction (XRPD). The X-ray powder diffraction spectra were collected on a Rigaku-Miniflex powder diffractometer using Cu−Kα (λ for Kα = 1.54059 Å) radiation obtained at 30 kV and 15 mA. The scans were run from 5.0° to 80.0° 2θ, increasing at a step size of 0.02° 2θ with a counting time of 5 s for each step.

Surface Area and Pore Diameter. The Brunauer−Emmett−Teller (BET) surface area and pore diameter of solid catalyst were determined from nitrogen adsorption−desorption measurement on ASAP2010 instrument (Micromeritics Instrument Corporation, Norcross, GA, USA). The samples were first evacuated at 393 K overnight before measurement. The pore size distributions were also calculated by the advanced Barrett−Joyner−Halenda (BJH) method using the adsorption−desorption branches of the isotherms.

Catalytic Activity Studies. The conversion of 2-phenyl-1,3-dioxolane to toluene was carried out at 53 °C in a batch reactor under H_2 balloon pressure in tetrahydrofuran (THF) solvent. In a typical experiment, 2-phenyl-1,3-dioxolane (0.15 g, 1 mmol) was added to a mixture of the tandem catalyst Pd/PSSH (40 mg, 16% Pd and 84% PSSH) in THF (10 mL). After 2 h reaction time at 53 °C, the reaction was stopped by cooling. Reactant and product concentrations were determined by gas chromatography (HP 5890, FID detector) with an Agilent HP-5 column (30 cm × 0.32 mm I.D.). Heptane was used as an internal standard. The catalytic activities of Pd/PSSH/Al_2O_3 and Pd/PSSH/TiO_2 were tested in the same manner as described above.

The conversion of phenol to cyclohexane was carried out at 200 °C using a Parr pressure reactor (300 mL), in aqueous medium under H_2 pressure. In a typical experiment, the supported tandem catalyst Pd/PSSH/TiO_2 (200 mg, 5% Pd and 26% PSS), phenol (1 g) and water (100 mL) were added to the Parr reactor, which was then purged with H_2 for 10 min, then charged with H_2 at 600 psi and sealed. The reactor was then heated at 200 °C for 4 h. The reaction was stopped by quench cooling. Ethyl acetate was added to extract the organic mixture. The organic mixture was analyzed by gas chromatography (HP 5890, FID detector) with an Agilent HP-5 column (30 cm × 0.32 mm I.D.) to determine the concentrations of reactant and final products. Heptane was used as an internal standard. The catalytic activity of M/PSSH/Al_2O_3, M = Pd, Pt, or Rh, was tested in the same manner as described above.

RESULTS AND DISCUSSION

Preparation of Tandem Catalyst. The route to synthesize Pd/PSSH/TiO_2 nanocomposite is illustrated in Figure 1. Water

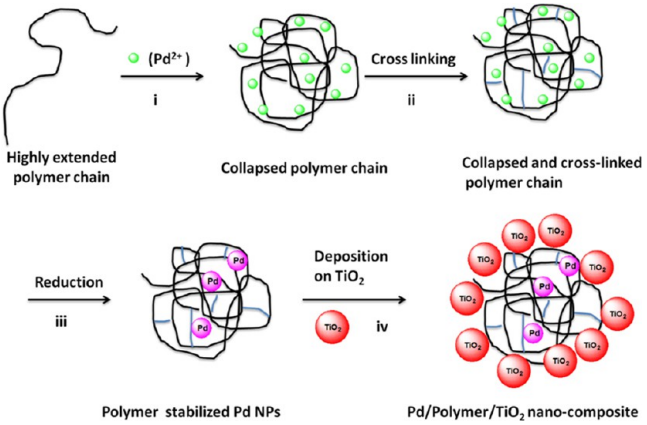

Figure 1. Synthesis of nanocomposite via counterion-induced polyelectrolyte collapse: (i) a solution of metal salt precursor (green dot) is added to a solution of extended polyelectrolyte to induce a chain-to-globule transition; (ii) the collapsed polymer chain is subjected to UV cross-linking; (iii) formation of Pd nanoparticles by $NaBH_4$ reduction (pink ball); (iv) deposition of nanocomposite on TiO_2 nanoparticles (red ball).

dispersible Pd nanoparticles were produced by using a polyelectrolyte collapse strategy. The polyelectrolyte PSS was partially ionized at aqueous solution with pH of 2−3 and existed as highly extended swollen chains arising from the repulsive electrostatic interactions along the chains. The

dx.doi.org/10.1021/sc400008e | ACS Sustainable Chem. Eng. 2013, 1, 381−388

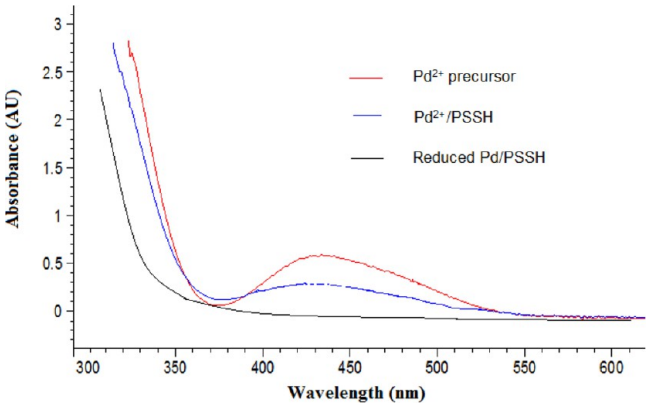

Figure 2. UV−vis spectra of Pd precursor and Pd/PSSH.

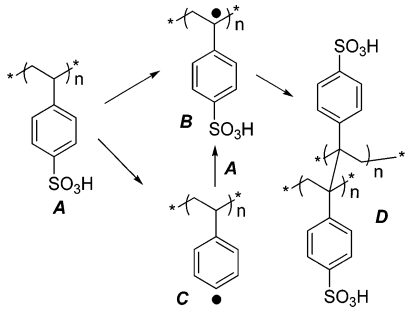

Figure 3. Acidic group loss mechanism of PSSH under UV irradiation and cross-linking by radical coupling.

Table 1. Effect of Cross-Linking Time on Loss of Acidic Group of PSSH

cross-linking time	reduction time	S wt %	loss of acidic group
1 h	1 h	11.4%	<1%
2 h	1 h	11.2%	<3%
3 h	1 h	9.9%	14%
4 h	1 h	8.1%	30%
5 h	1 h	6.8%	41%
PSSH		11.5%	0

addition of palladium(II) in aqueous solution caused a transition from extended-chain to collapsed-globule. Cross-linking the collapsed polymer chains under UV with a wavelength of 254 nm resulted in a rigid polymer template, in which palladium(II) was encapsulated.[33,34] The trapped palladium(II) was then reduced by $NaBH_4$ to form Pd nanoparticles. UV−vis spectra shown in Figure 2 clearly revealed the absence of the absorbance peak at 460 nm of the palladium(II) precursor solution upon the reduction to water-dispersed Pd nanoparticles. Finally, the Pd/PSSH nanocomposite was coprecipitated with TiO_2 and Al_2O_3 to give the heterogeneous catalysts Pd/PSSH/TiO_2 and Pd/PSSH/Al_2O_3, respectively.

Effect of the Cross-Linking Time on the Acidic Groups of PSSH. The main goal of cross-linking of polymer under UV irradiation is to stabilize the globule structure of polymer to encapsulate the Pd nanoparticles. However, the radicals generated by UV can react with oxygen, resulting in oxidation which ultimately causes degradation of the polymers when the irradiation is conducted under oxygen. The cross-linking time is also crucial to the integrity of the polymer. Since the nanocomposite is expected to be used as a tandem catalyst, it

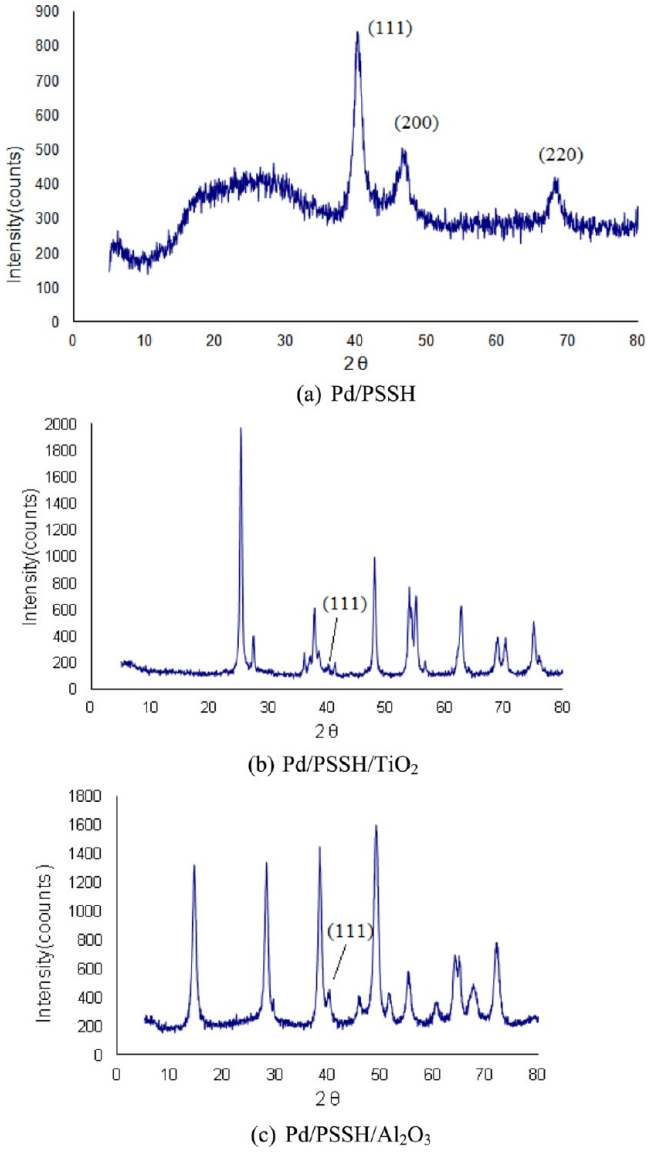

Figure 4. XRD patterns of Pd/PSSH, Pd/PSSH/TiO_2, and Pd/PSSH/Al_2O_3.

is desirable to keep the activity of Pd, and also the acidity of PSSH, at a maximum level.

There are two likely mechanisms of cross-linking of PSSH as shown in Figure 3. Photochemical cross-linking of polystyrene derivatives typically occurs by α-hydrogen abstraction which converts the linear polymer, **A**, to the tertiary radicals **B**, which then couple to form the cross-linked polymer **D**. However, PSSH can also undergo cleavage of the sulfonic acid group, to give a very shortlived aryl radical **C**.[35] This aryl radical can abstract an α-hydrogen from PSSH to give a second route to the tertiary radical **B** and hence to the cross-linked polymer **D**. Only the acidic group cleavage causes loss of acidity of the polymers, and must be minimized in order to retain the solid acid property of the polymer. The cross-linking process was performed under the protection of nitrogen to minimize the degradation of PSSH caused by oxidation of intermediate radicals. Additionally, the loss of the acidic sulfonic acid group with time was monitored through measuring the sulfur content of the material by XPS, and results are listed in Table 1. The XPS technique probes to a depth of 10−15 nm, so it can give

dx.doi.org/10.1021/sc400008e | ACS Sustainable Chem. Eng. 2013, 1, 381−388

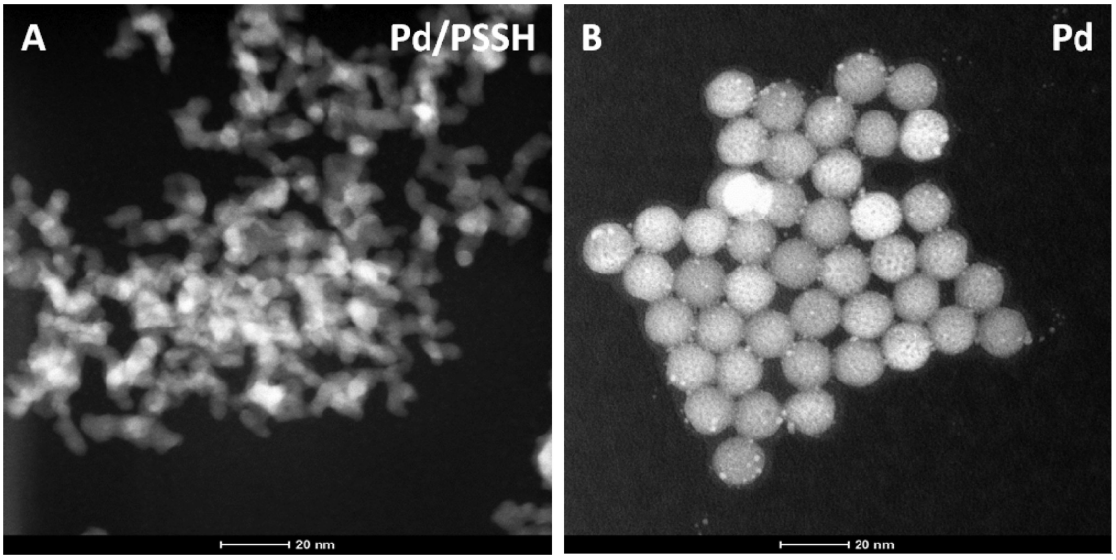

Figure 5. TEM images of Pd particles in Pd/PSSH: without (left) and with (right) plasma cleaning.

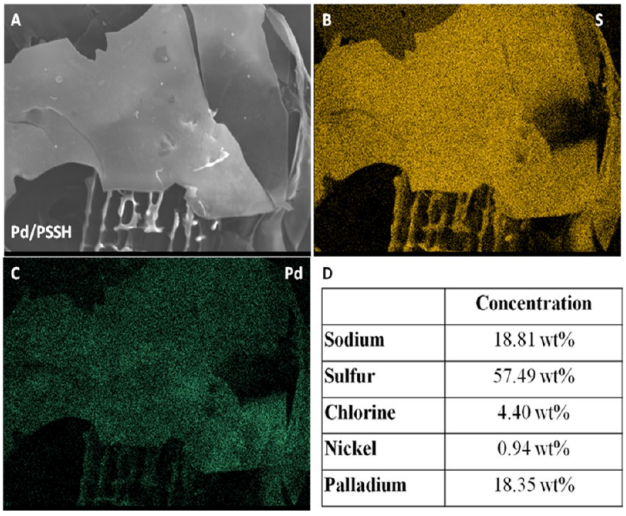

	Concentration
Sodium	18.81 wt%
Sulfur	57.49 wt%
Chlorine	4.40 wt%
Nickel	0.94 wt%
Palladium	18.35 wt%

Figure 6. SEM image of the area where EDX mapping was undertaken for Pd and S of Pd/PSSH: (A) SEM image of original surface; (B) elemental distribution of S; (C) elemental distribution of Pd; (D) EDX analysis of the surface.

Table 2. BET Results for the Catalysts

catalyst	BET specific surface area (m^2/g)	pore diameter (nm)
Pd/PSSH	9.9	3.3
Pd/PSSH/TiO_2	57.1	8.9
Pd/PSSH/Al_2O_3	83.4	16.4

reliable analysis for these porous materials. The results show that within the 2 h cross-linking time the acidic group loss can be controlled to be less than 3% while the Pd/PSSH remains as a stable dispersion in solution.

Characterization of the Nanocomposites. *XRD.* Figure 4 shows the X-ray diffraction patterns of Pd/PSSH, Pd/PSSH/TiO_2, and Pd/PSSH/Al_2O_3. As shown in Figure 4a, Pd in Pd/PSSH showed XRD characteristic diffraction peaks at 2θ = 39.4°, 45.68°, 66.84°, which were assigned to (111), (200), and (220) crystalline planes of faced centered cubic structured palladium.[36] After Pd/PSSH was deposited on supports Al_2O_3 and TiO_2, most characteristic peaks of Pd were suppressed by dominant characteristic peaks of Al_2O_3 (2θ = 14.5°, 28.2°, 38.4°, 45.9°, 49.1°, 51.8°, 55.2°, 60.6°, 64.1°, 67.4°, 72.1°) and TiO_2 (2θ = 25.3°, 28.2°, 36.1°, 37.8°, 41.3°, 48.1°, 53.9°, 55.1°, 62.7°, 70.3°, 75.1°,82.5°) as illustrated in Figure 3b and c. The characteristic peak of Pd at 2θ of 39.4° corresponding to (111) crystalline plane, are still visible, which is distinguished from any characteristic peaks of Al_2O_3 and TiO_2. The XRD results indicated that Pd remained in a metallic state after it was deposited on the metal oxide supports.

TEM. The transmission electron microscopy images of the nonstained nanocomposite in Figure 5 revealed that Pd nanoparticles were uniformly distributed onto the polymer network. The average particle size of spherical Pd nanoparticles was 13 nm.

SEM. Additional evidence for the successful incorporation and uniform distribution of Pd nanoparticles in PSSH capsules was provided by elemental mapping using energy dispersive X-ray spectroscopy (Figure 6). Uniform distributions of S and Pd can be seen in Figure 6B and C. The EDX analysis of sulfur and palladium is shown in Figure 6D.

BET Analysis. The specific surface areas of the tandem catalysts were measured by Brunauer–Emmett–Teller (BET) nitrogen adsorption after degassing at 120 °C for 16 h. The results are summarized in Table 2. The surface area of original Pd/PSSH was found to be 9.9 m^2/g. The Pd/PSSH/TiO_2 and Pd/PSSH/Al_2O_3 composites had surface areas of 57 and 83.4 m^2/g. The surface area of Pd/PSSH/Al_2O_3 was much less than the original surface area of Al_2O_3 (130 m^2/g), which indicates that some of Al_2O_3 nanoparticles were aggregated under the acidic conditions. In contrast, the surface area of Pd/PSSH/TiO_2 was very close to the initial surface area of TiO_2 (50 m^2/g), indicating that the surface area of the TiO_2 support has been well preserved. Less aggregation of TiO_2 also indicates a uniform dispersion of Pd on the TiO_2 support, and therefore, a better catalytic activity was expected from Pd/PSSH/TiO_2.

XPS Analysis. The chemical states of Pd in tandem catalyst were also characterized by XPS, and the results are shown in Figure 7. It can be seen that the Pd 3d spectrum could be resolved into two spin–orbit pairs with $3d_{5/2}$ binding energies of 335.2 and 336.9 eV, respectively. The peak binding energies of 335.2 eV (Pd $3d_{5/2}$) and 340.5 eV (Pd $3d_{3/2}$) correspond to

dx.doi.org/10.1021/sc400008e | ACS Sustainable Chem. Eng. 2013, 1, 381–388

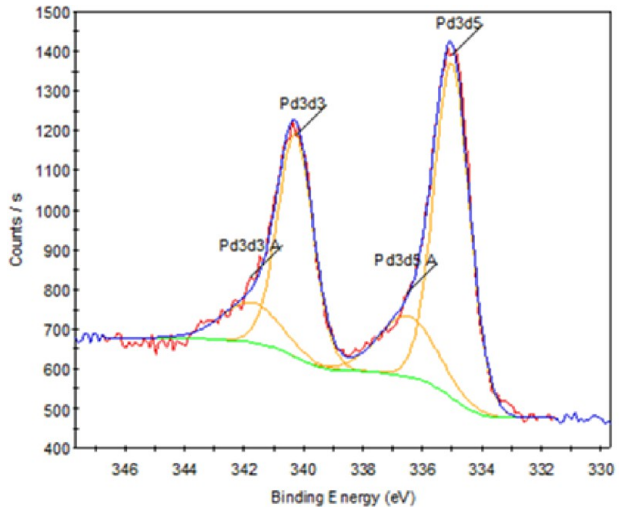

Pd wt%	Pd/PSSH	Pd/PSSH/TiO_2	Pd/PSSH/Al_2O_3
Pd^{n+}	80	29	20
Pd^0	20	71	80

Figure 7. XPS analytical results for the three tandem catalysts.

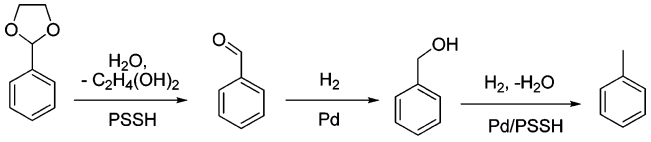

Figure 8. Model tandem reaction carried out at 53 °C, showing the likely active catalyst for each step.

fully reduced Pd^0 nanoparticles, while the peak at 336.9 eV ($3d_{5/2}$) and 342.2 eV ($3d_{3/2}$) suggest the presence of some nonzerovalent palladium (Pd^{n+}).[37] This result shows that not all of the palladium(II) was reduced to palladium(0), probably due to the acidic environment.[38] The residual palladium(II) should be easily reduced to palladium(0) in the catalytic hydrogenation reaction under hydrogen atmosphere. Interestingly, as shown in Figure 7, the weight percent of Pd^0 in the catalysts with supports is much higher than that of Pd/PSSH without any support, which indicates that Pd^0 can be significantly stabilized by the oxide supports. In addition, we found that Pd^0 is more stable on Al_2O_3 support than on TiO_2 support, presumably because Al_2O_3 is less acidic than TiO_2.

Performance of the Three Catalysts in a Model Tandem Reaction. The three catalysts, Pd/PSSH, Pd/PSSH/TiO_2, and Pd/PSSH/Al_2O_3, were tested in a model tandem reaction to convert 2-phenyl-1,3-dioxolane to toluene. This targeted reaction involves three sequential steps, namely deprotection by hydrolysis, hydrogenation, and hydrogenation/dehydration as shown in Figure 8. This tandem reaction uses acid catalyst and palladium catalyst respectively in the first and the second step while involving both catalysts in the third step, which makes this reaction an excellent model reaction to demonstrate the concept of tandem catalysis.

Table 4. Activity of the Catalysts in Phenol Conversion[a]

catalyst	Pd loading with respect to the starting material (wt %)	conversion: phenol %	yield: cyclohexane %
Pd/PSSH/Al_2O_3	1.0%	91%	46%
Pd/PSSH/TiO_2	1.0%	98%	78%

[a]Reaction time 4 h; temperature 200 °C; hydrogen pressure 600 psi; solvent is water.

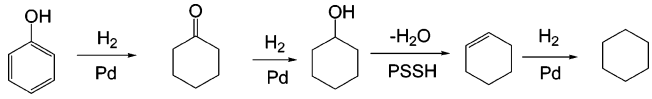

Figure 9. Hydrodeoxygenation of phenol, showing the likely active catalyst for each step.

Table 3 summarizes the conversion of the reactant 2-phenyl-1,3-dioxolane and the yields of the intermediates and the final product toluene using the three different catalysts. No other byproducts were detected by GC analysis. The nanocomposite Pd/PSSH/TiO_2 exhibited the highest catalytic activity in this reaction. Conversion of 2-phenyl-1,3-dioxolane was 94% and yield of toluene was 58% within a 2 h reaction time at 53 °C. Pd/PSSH/Al_2O_3 gave a lower conversion due to the amphoteric nature of Al_2O_3, which resulted in lower activities in the two acid-catalyzed steps. Poor performance of Pd/PSSH with 25.6% conversion of 2-phenyl-1,3-dioxolane and 7% yield of toluene under the same catalyst loading may result from its small surface area as well as the difficulty in mixing with organic solvent due to the fluffy nature of the Pd/PSSH powder. These results suggest that the supports like TiO_2 and Al_2O_3 not only

Table 3. Catalytic Activity of Catalysts in Model Tandem Reaction[a]

catalyst	Pd loading with respect to the starting material (wt %)	conversion: 2-phenyl-1,3-dioxolane %	yield: PhCH=O %	yield: $PhCH_2OH$ %	yield: $PhCH_3$ %
Pd/PSSH	4.2%	25.6%	7%	1.2%	7%
Pd/PSSH/Al_2O_3	4.2%	54%	10%	0.2%	37%
Pd/PSSH/TiO_2	4.2%	94%	19%	4.5%	58%

[a]Reaction time 2 h; temperature 53 °C; hydrogen pressure is slightly higher than 1 atm; solvent is THF.

dx.doi.org/10.1021/sc400008e | ACS Sustainable Chem. Eng. 2013, 1, 381−388

stabilize Pd(0) nanoparticles[39] but also provide adsorption sites for the reactants, which greatly improve the catalytic efficiency. Without such supports, the performance of Pd/PSSH is lower.

For such metal/polymer nanocomposite catalysts to function well, it is important that the Pd nanoparticles did not diffuse out from the polymer template into solvent, during the reaction. This was confirmed by testing the Pd content in the resulting solution after reaction by ICP. No detectable amount of palladium was leached into the solution, as probed by ICP analysis, and the catalyst recovered by filtration reproducibly retained its activity to a level greater than 90% over at least three cycles. Experiments were also carried out using Pd and PSSH separately as catalysts, but no toluene was formed in either case. Hence it is demonstrated that the Pd/PSSH nanocomposite is acting as a tandem catalyst in converting 2-phenyl-1,3-dioxolane to toluene and that it acts as a true heterogeneous catalyst in this reaction.

Application of the Catalysts Pd/PSSH/TiO_2 and Pd/PSSH/TiO_2 in Bio-Oil Upgrading. Bio-oil obtained by pyrolysis and liquefaction cannot be used directly as a transportation fuel due to its high oxygen content, and related low stability and low heating value. Upgrading through hydrodeoxygenation (HDO) is a necessary downstream step for the wider use of bio-oil.[40−43] Having demonstrated that Pd/PSSH/TiO_2 and Pd/PSSH/Al_2O_3 are capable of catalyzing a model metal-mediated hydrogenation reaction and acid-mediated dehydration reaction in tandem, it was considered that the catalyst may have the potential to upgrade bio-oil through a one-pot HDO process. We used phenol as a model compound to evaluate the activity of these catalysts in the conversion of phenol to cyclohexane.[44−47] The results are listed in Table 4.

As shown in Table 4, high phenol conversion of 98% and moderate yield of cyclohexane of 78% were obtained reproducibly under mild reaction conditions by Pd/PSSH/TiO_2. This HDO process is efficient, inherently green, and environmentally friendly. It has a number of advantages over the conventional HDO process,[48] such as minimizing the concerns of acid corrosion through using a solid acid PSSH instead of a liquid acid, reducing the cost associated with the product purification/separation through one-pot process, and increasing the catalytic efficiency by employing nanoscale Pd particles.

Arene hydrogenation, in the presence of functional groups, is challenging,[44−47,49−51] and we have also investigated this reaction with the analogous Pt/PSSH/Al_2O_3 and Rh/PSSH/Al_2O_3. The catalytic activity, as measured by the conversion to cyclohexane using the conditions of Table 4, followed the sequence Rh (81%) > Pd (46%) > Pt (5%), consistent with the known high reactivity of rhodium nanoparticles in arene hydrogenation.[49−51]

CONCLUSIONS

In summary, we have prepared Pd/PSSH nanocomposites supported on metal oxides with both basic (alumina) and acidic (titania) properties via a novel polyelectrolyte collapse strategy, and the catalyst materials have been characterized by several analytical methods. This kind of nanocomposite demonstrated a high catalytic activity in a model tandem reaction under mild conditions. The preparation of Pd/PSSH nanocomposites in aqueous media provides a simple, scalable, and environmentally friendly method that can be applied to the synthesis of a number of metal/functional polymer nanocomposites. The supported catalysts are resistant to leaching of the palladium nanoparticles, and the catalysts can easily be recovered and reused.[52] Hence, nanocomposites prepared by this method have promise as tandem catalysts for applications of academic and industrial significance, which require both a metal catalyst and a strong acid to catalyze individual steps.[1−34] The catalysts have potential use in the upgrading of biofuels and in other reactions that require both hydrogenation and deoxygenation of organic compounds.

AUTHOR INFORMATION

Corresponding Author

*E-mail: pudd@uwo.ca.

Present Address

⊥T.T.I.: Division of Physical Sciences and Engineering, Solar and Photovoltaics Engineering Center, King Abdullah University of Science and Technology (KAUST), Thuwal 23955−6900, Saudi Arabia.

Notes

The authors declare no competing financial interest.

ACKNOWLEDGMENTS

We thank the NSERC (Canada) for financial support.

REFERENCES

(1) Zanardi, A.; Mata, J. A.; Peris, E. Well-defined Ir/Pd complexes with a triazolyl-diylidene bridge as catalysts for multiple tandem reactions. *J. Am. Chem. Soc.* **2009**, *131*, 14531−14537.

(2) Ajamian, A.; Gleason, J. L. Two birds with one metallic stone: Single-pot catalysis of fundamentally different transformations. *Angew. Chem., Int. Ed.* **2004**, *43*, 3754−3760.

(3) Dai, Y.; Wensink, P. C.; Abeles, R. H. One protein, two enzymes. *J. Biol. Chem.* **1999**, *274*, 1193−1195.

(4) Ju, T.; Goldsmith, R. B.; Chai, S. C.; Maroney, M. J.; Pochapsky, S. S.; Pochapsky, T. C. One protein, two enzymes revisited: A structural entropy switch interconverts the two isoforms of acireductone dioxygenase. *J. Mol. Biol.* **2006**, *363*, 823−834.

(5) Kjellen, L.; Pettersson, I.; Unger, E.; Lindahl, U. Two enzymes in one: N-deacetylation and N-sulfation in heparin biosynthesis are catalyzed by the same protein. *Adv. Exp. Med. Biol.* **1992**, *313*, 107−111.

(6) Liao, J.; Maulide, N.; Augustyns, B.; Markó, I. E. Tandem radical rearrangement/Pd-catalysed translocation of bicyclo[2.2.2]lactones. An efficient access to the oxa-triquinane core structure. *Org. Biomol. Chem.* **2006**, *4*, 1464−1467.

(7) Landge, S. M.; Schmidt, A.; Outerbridge, V.; Török, B. Synthesis of pyrazoles by a one-pot tandem cyclization-dehydrogenation approach on Pd/C/K-10 catalyst. *Synlett* **2007**, 1600−1604.

(8) Yamada, Y.; Tsung, C.; Huang, W.; Huo, Z.; Habas, S. E.; Soejima, T.; Aliaga, C. E.; Somorjai, G. A.; Yang, P. Nanocrystal bilayer for tandem catalysis. *Nature Chem.* **2011**, *3*, 372−376.

(9) Sharma, K. K.; Biradar, A. V.; Das, S.; Asefa, T. Bifunctional mesoporous silica catalyst for C-C bond forming tandem reactions. *Eur. J. Inorg. Chem.* **2011**, 3174−3182.

(10) Shiju, N. R.; Alberts, A. H.; Khalid, S.; Brown, D. R.; Rothenberg, G. Mesoporous silica with site-isolated amine and phosphotungstic acid groups: A solid catalyst with tunable antagonistic functions for one-pot tandem reactions. *Angew. Chem., Int. Ed.* **2011**, *50*, 9615−9619.

(11) Terashima, T.; Nomura, A.; Ito, M.; Ouchi, M.; Sawamoto, M. Star-polymer-catalyzed living radical polymerization: Microgel-core reaction vessel by tandem catalyst interchange. *Angew. Chem., Int. Ed.* **2011**, *50*, 7892−7895.

(12) Yang, M.; Yan, W.; Hao, X.; Liu, B.; Wen, L.; Liu, P. Tandem catalytic systems: One catalyst combined with two different activators

for preparing branched polyethylene with ethylene as single monomer. *Macromolecules* **2009**, *42*, 905−907.
(13) Pijnenburg, N. J. M.; Dijkstra, H. P.; van Koten, G.; Gebbink, R. J. M. K. SCS-pincer palladium-catalyzed auto-tandem catalysis using dendritic catalysts in semi-permeable compartments. *Dalton Trans.* **2011**, *40*, 8896−8905.
(14) Li, J.; Siegler, M.; Lutz, M.; Spek, A. L.; Gebbink, R. J. M. K.; van Koten, G. PCN- and PCS-pincer palladium complexes as tandem catalysts in homoallylation reactions. *Adv. Synth. Catal.* **2010**, *352*, 2474−2488.
(15) Raluy, E.; Favier, I.; López-Vinasco, A. M.; Pradel, C.; Martin, E.; Madec, D.; Teuma, E.; Gómez, M. A smart palladium catalyst in ionic liquid for tandem processes. *Phys. Chem. Chem. Phys.* **2011**, *13*, 13579−13584.
(16) Murata, T.; Murai, M.; Ikeda, Y.; Miki, K.; Ohe, K. Pd- and Cu-catalyzed one-pot multicomponent synthesis of hetero α,α'-dimers of heterocycles. *Org. Lett.* **2012**, *14*, 2296−2299.
(17) Arnanz, A.; Pintado-Sierra, M.; Sanchez, F. Bifunctional metal organic framework catalysts for multistep reactions: MOF-Cu(BTC)-[Pd] catalyst for one-pot heteroannulation of acetylenic compounds. *Adv. Synth. Catal.* **2012**, *354*, 1347−1355.
(18) Jiang, C.; Covell, D. J.; Stepan, A. F.; Plummer, M. S.; White, M. C. Sequential allylic C-H amination/vinylic C-H arylation: A strategy for unnatural amino acid synthesis from a-olefins. *Org. Lett.* **2012**, *14*, 1386−1389.
(19) Wu, H.; He, Y. P.; Gong, L. Z. The combination of relay and cooperative catalysis with a gold/palladium/Bronsted acid ternary system for the cascade hydroamination/allylic alkylation reaction. *Adv. Synth. Catal* **2012**, *354*, 975−980.
(20) Afewerki, S.; Ibrahem, I.; Rydfjord, J.; Breistein, P.; Cordova, A. Direct regiospecific and highly enantioselective intermolecular a-allylic alkylation of aldehydes by a combination of transition-metal and chiral amine catalysts. *Chem.—Eur. J.* **2012**, *18*, 2972−2977.
(21) Lira, R.; Wolfe, J. P. Palladium-catalyzed synthesis of N-aryl-2-benzylindolines via tandem arylation of 2-allylaniline: Control of selectivity through in situ catalyst modification. *J. Am. Chem. Soc.* **2004**, *126*, 13906−13907.
(22) Bergbreiter, D. E.; Kippenberger, A.; Zhong, Z. Catalysis with palladium colloids supported in poly(acrylic acid)-grafted polyethylene and polystyrene. *Can. J. Chem.* **2006**, *84*, 1343−1350.
(23) Ohtaka, A.; Tamaki, Y.; Igawa, Y.; Egami, K.; Shimomura, O.; Nomura, R. Polyion complex stabilized palladium nanoparticles for Suzuki and Heck reaction in water. *Tetrahedron* **2010**, *66*, 5642−5646.
(24) Smuleac, V.; Bachas, L.; Bhattacharyya, D. Aqueous-phase synthesis of PAA in PVDF membrane pores for nanoparticle synthesis and dichlorobiphenyl degradation. *J. Membr. Sci.* **2010**, *346*, 310−317.
(25) Jiang, Y. J.; Gao, Q. M. Heterogeneous hydrogenation catalyses over recyclable Pd(0) nanoparticle catalysts stabilized by PAMAM-SBA-15 organic-inorganic hybrid composites. *J. Am. Chem. Soc.* **2006**, *128*, 716−717.
(26) Gopidas, K. R.; Whitesell, J. K.; Fox, M. A. Synthesis, characterization, and catalytic applications of a palladium-nanoparticle-cored dendrimer. *Nano Lett.* **2003**, *3*, 1757−1760.
(27) Scott, R. W. J.; Wilson, O. M.; Crooks, R. M. Synthesis, characterization, and applications of dendrimer-encapsulated nanoparticles. *J. Phys. Chem.* **2005**, *109*, 692−704.
(28) Mayer, A. B. R.; Mark, J. E. Transition metal nanoparticles protected by amphiphilic block copolymers as tailored catalyst systems. *Colloid Polym. Sci.* **1997**, *275*, 333−340.
(29) Lu, Z. H.; Liu, G. J.; Phillips, H.; Hill, J. M.; Chang, J.; Kydd, R. A. Palladium nanoparticle catalyst prepared in poly(acrylic acid)-lined channels of diblock copolymer microspheres. *Nano Lett.* **2001**, *1*, 683−687.
(30) Narayanan, R.; El-Sayed, M. A. Effect of catalysis on the stability of metallic nanoparticles: Suzuki reaction catalyzed by PVP-palladium nanoparticles. *J. Am. Chem. Soc.* **2003**, *125*, 8340−8347.
(31) Campbell, D. J.; Miller, J. D.; Andersh, B. J. Synthesis of palladium colloids within polydimethylsiloxane and their use as catalysts for hydrogenation. *J. Colloid Interface Sci.* **2011**, *360*, 309−312.
(32) Wei, Y.; Soh, S.; Apodaca, M. M.; Kim, J.; Grzybowski, B. A. Sequential reactions directed by core/shell catalytic reactors. *Small* **2010**, *6*, 857−863.
(33) Goh, C. M.; Dinglasan, J. A.; Goh, J. B.; Loo, R.; Veletanlic, E. *Composite nanoparticles, nanoparticles, and methods for producing same*. US Pat. 7 534 490, 2009.
(34) Anderson, D.; Dinglasan, J. A.; Loukine, N. *Producing nanoparticles using nanoscale polymer template*. US Pat. 7 645 318, 2010.
(35) Hong, K.; Kim, S. H.; Yang, C.; Yun, W. M.; Nam, S.; Jang, J.; Park, C.; Park, C. E. Photopatternable poly(4-styrene sulfonic acid)-Wrapped MWNT thin-film source/drain electrodes for use in organic field-effect transistors. *ACS Appl. Mater. Interfaces* **2011**, *3*, 74−79.
(36) Xu, L.; Wu, X. C.; Zhu, J. J. Green preparation and catalytic application of Pd nanoparticles. *Nanotechnology* **2008**, *19*, 305603 (6 pp).
(37) Chun, Y. S.; Shin, J. Y.; Song, C. E.; Lee, S.-G. Palladium nanoparticles supported onto ionic carbon nanotubes as robust recyclable catalysts in an ionic liquid. *Chem. Commun.* **2008**, 942−944.
(38) Ferreira, P. J.; La O', G. J.; Shao-Horn, Y.; Morgan, D.; Makharia, R.; Kocha, S.; Gasteiger, H. A. Instability of Pt/C electrocatalysts in proton exchange membrane fuel cells: A mechanistic investigation. *J. Electrochem. Soc.* **2005**, *152*, A2256−A2271.
(39) Cirtiu, C. M.; Dunlop-Brière, A. F.; Moores, A. Cellulose nanocrystallites as an efficient support for nanoparticles of palladium: Application for catalytic hydrogenation and Heck coupling under mild conditions. *Green Chem.* **2011**, *13*, 288−291.
(40) Manzer, L. E. Recent developments in the conversion of biomass to renewable fuels and chemicals. *Top. Catal.* **2010**, *53*, 1193−1196.
(41) Mortensen, P. M.; Grunwaldt, J. D.; Jensen, P. A.; Knudsen, K. G.; Jensen, A. D. A review of catalytic upgrading of bio-oil to engine fuels. *Appl. Catal., A* **2011**, *407*, 1−19.
(42) Gallezot, P. Conversion of biomass to selected chemical products. *Chem. Soc. Rev.* **2012**, *41*, 1538−1558.
(43) Tuck, C. O.; Prez, A.; Horvath, I. T.; Sheldon, R. A.; Poliakoff, M. Valorization of biomass: Deriving more value from waste. *Science* **2012**, *337*, 695−699.
(44) Mori, K.; Furubayashi, K.; Okada, S.; Yamashita, Y. Unexpected Pd-catalyzed hydrogenation of phenol to 2-cyclohexene-1-one: enhanced activity and selectivity assisted by molecular oxygen. *Chem. Commun.* **2012**, *48*, 8886−8888.
(45) Liu, H.; Jiang, T.; Han, B.; Liang, S.; Zhou, Y. Selective phenol hydrogenation to cyclohexanone over a dual supported Pd-Lewis acid catalyst. *Science* **2009**, *326*, 1250−1252.
(46) Wang, Y.; Yao, J.; Li, H. R.; Su, D. S.; Antonietti, M. Highly selective hydrogenation of phenol and derivatives over a Pd@carbon nitride catalyst in aqueous media. *J. Am. Chem. Soc.* **2011**, *133*, 2362−2365.
(47) Foster, A. J.; Do, P. T. M.; Lobo, R. F. The synergy of the support acid function and the metal function in the catalytic hydrodeoxygenation of *m*-cresol. *Top. Catal.* **2012**, *55*, 118−128.
(48) Zhao, C.; Kou, Y.; Lemonidou, A. A.; Li, X. B.; Lercher, J. A. Highly selective catalytic conversion of phenolic bio-oil to alkanes. *Angew. Chem., Int. Ed.* **2009**, *48*, 3987−3990.
(49) Stratton, S. A.; Luska, K. L.; Moores, A. Rhodium nanoparticles stabilized with phosphine functionalized imidazolium ionic liquids as recyclable arene hydrogenation catalysts. *Catal. Today* **2012**, *183*, 96−100.
(50) Baumgartner, R.; McNeill, K. Hydrodefluorination and hydrogenation of fluorobenzene under mild aqueous conditions. *Environ. Sci. Technol.* **2012**, *46*, 10199−10205.
(51) Debouttiere, P. J.; Coppel, Y.; Denicourt-Nowicki, A.; Roucoux, A.; Chaudret, B.; Philippot, K. PTA-stabilized ruthenium and platinum nanoparticles: Characterization and investigation in aqueous biphasic hydrogenation catalysis. *Eur. J. Inorg. Chem.* **2012**, 1229−1236.

(52) Pachon, L. D.; Rothenberg, G. Transition-metal nanoparticles: synthesis, stability and the leaching issue. *Appl. Organomet. Chem.* **2008**, *22*, 288.